Int. J. Electrochem. Sci., 8 **(2013)** 8167 - 8174

International Journal of
ELECTROCHEMICAL
SCIENCE
www.electrochemsci.org

Size Effect of Heterostructure Type in Core/Shell Quantum Dot

Guozhi Jia[1,3,*], *Bingxue Hao*[2], *Xucen Lu*[2], *Jianghong Yao*[2]

[1]Tianjin Institute of Urban Construction, Tianjin 300384, China
[2]The Key Laboratory of Advanced Technique and Fabrication for Weak-Light Nonlinear Photonics Materials, Ministry of Education, Nankai University, Tianjin 300457, China
[3]Institute of Semiconductors, Chinese Academy of Sciences, P.O. Box 912, Beijing 100083, China
[*]E-mail: gzjia@semi.ac.cn

Received: 6 April 2013 / *Accepted:* 29 April 2013 / *Published:* 1 June 2013

Size effect of heterostructure type and exciton properties in $ZnTe_xSe_{1-x}$/ZnSe core/shell structure QDs have been investigated by effective-mass approximation method with taking into the Coulomb interaction account. The heterostructure types of QDs can be changed from Type-I, to Type-II with changing of the size of QDs. The spatial separation between electron and hole in QDs can be presence abruptly by adjusting Se molar fraction in the core region and size of QDs. We demonstrate that the quantum confinement effect in the ternary core is a key to the transformation from the type-I to type- II. The transition energies can be widely tuned by the changing the Se molar fraction in the core layer and size of QDs.

Keywords: Heterostructure; Exciton properties; Core/shell; Quantum dot; Size effect

1. INTRODUCTION

Semiconductor nanocrystals (NCs) have attracted much recent research interest due to its potential application in light-emitting devices [1], biological tagging materials [2-5], and solar cell [6]. Particularly important in NCs is to find emission peak tuning wildly and extending to long wavelength, for example NIR wavelengths. Doping can be a method to realize the emission wavelength, which can result in deteriorating the optical properties. Cd-free QDs were proved their potentials toward "nontoxic" biological or medical applications that are free from concerns regarding heavy-metal leakage [7]. As for Zn-based QDs, growth habit itself result in the low luminous efficiency. To date, a type-I to type-II band alignment transition is reported by varying the InAsSb composition from pure InAs to InSb, which develop a means to tailoring the band structure [8]. Contrary to type-I, type-II structure QDs alignment spatially separate carriers into the two different range of the core and shell

due to the lowest energy states for electrons and holes in the different layer of QDs. This can be engineered to emit longer wavelength than one of either semiconductor comprising QDs [7]. The effective band gaps of type-II structure QDs is smaller than the energy gap of the core and shell materials and mainly determined by the band offsets and size of the core and shell. The spatial separation of carriers in the type-II structure QDs provides new means of controllable wavefunction and makes these structures QDs be beneficial for photovoltaic or photoconduction applications. Additionally, the Auger and radiative decay lifetime can be slowed due to the excitons separated in the different areas of the type-II structure QDs [9].

Compared with the binary semiconductor compounds structure, the QDs with a ternary semiconductor compound structure can produce a new degree of freedom for tailoring the band structure. More theoretical study have showed the effective mass approximation (EMA) is an important method to theoretically research the quantum confinement effect of the core/shell QDs[7]. The EMA can be applied to calculate the electronic and optical properties, such as, the electron and hole wave functions, the transition energy, and the overlap of the wave functions et al. Chang *et al*. pointed out that the spatially separated characteristic of electron and hole can be enhanced significantly in QDQW with the two wells [11]. They systematically investigated the electron and hole wave functions, the 1*s* transition energy, and the overlap of the wave functions.

In this paper, we present a type-I to type-II band alignment transition by varying the size of QDs and Se molar composition in the ternary semiconductor core/shell structure QDs. The simple EMA model was used to study the exciton energy, and overlap integral in $ZnTe_xSe_{1-x}$/ZnSe core/shell QDs with taking into the Coulomb interaction account. The electron and hole wave functions, the 1*s* transition energy, and the overlap of the wave functions is analyzed. The transition mechanism between type-I and type-II is also discussed.

2. THEORY

We assume that the QDs were placed in an infinite potential well. When the space-dependent effective mass of carriers is taken into account, the Schrodinger equation of carriers in the framework of the single-band effective mass approximation in the QDs region is as follows[7,10-12]:

$$\left(-\frac{\hbar^2}{2}\nabla\frac{1}{m_i}\nabla - V(r)\right)\Psi(r) = E\Psi(r) \qquad (1)$$

where $\hbar$ is Planck's constant divided by 2π, m_i and $V(r)$ the particle mass and a potential depending on the position in the QDs, E the energy eigenvalue, and $\psi(r)$ the corresponding eigenfunction. Here, we consider QDs with spherically symmetric structure and homogeneous potentials, which leads to separate the wave functions into the radial and angular parts as follows:

$$\Psi_{nlm}(r,\theta,\phi) = R_{nl}(r)Y_{lm}(\theta,\phi) \qquad (2)$$

$R_{nl}(r)$ is the radial wave function, and $Y_{lm}(\theta,\phi)$ a spherical harmonic. n is the principal quantum number, and l and m are the angular momentum numbers. We shall restrict the calculations to

1*s* states for $n=1$, $l=m=0$. We obtain the solutions for QDs by solving the continuity relations of the carriers wave functions and the probability currents at the boundaries:

$$R_{nl,i}(k_i r_i) = R_{nl,i+1}(k_{i+1} r_i) \quad (3)$$

$$\frac{1}{m_i}\frac{dR_{nl,i}(k_i r_i)}{dr}\bigg|_{r=r_i} = \frac{1}{m_{i+1}}\frac{dR_{nl,i+1}(k_{i+1} r_i)}{dr}\bigg|_{r=r_i} \quad (4)$$

where $k_{i/i+1} = \left[\frac{2m_i(E-V)}{\hbar^2}\right]^{1/2}$ is the wave vectors in core and shell, respectively, $R_{nl,i}(r_i)$ and $R_{nl,i+1}(r_i)$ are the radial wave functions for the carriers (electron or hole) in the core and shell, respectively, m_i and m_{i+1} are the carrier effective masses in the core and shell, respectively.

The Coulomb interaction energy between electron and hole pair can be treated as a heliumlike perturbation according to the first-order perturbation approximation. After expanding of $1/|r_e - r_h|$ in spherical harmonics form and integrating the angular coordinates, the Coulomb interaction energy can be expressed as

$$E_c = -\frac{e^2}{4\pi\varepsilon_0}\iint dr_e dr_h r_e^2 r_h^2 \frac{|R_e(r_e)|^2 |R_h(r_h)|^2}{\max(r_e, r_h)\bar{\varepsilon}(r_e, r_h)} \quad (5)$$

As for conduction-band positions of ternary ZnTeSe, linear interpolation between the binary materials is used in the simulation. The valence band potential has a nonlinear dependence on composition due to "optical band-bowing", and can be expressed as follows:

$$E^0_{v,ZnTeSe} = xE^0_{v,ZnTe} + (1-x)E^0_{v,ZnSe} + 3x(1-x)(a_v^{ZnSe} - a_v^{ZnTe})\frac{a_{ZnTe} - a_{ZnSe}}{a_{ZnTeSe}} \quad (6)$$

where the parameter a_v represents the hydrostatic deformation potential for the valence band. where the lattice constant ternary semiconductor $a_{ZnTeSe} = (1-x)a_{ZnSe} + xa_{ZnTe}$. For ternary semiconductor compound, the optical band-gap was given using bowing parameters:

$$E_{g,ZnTeSe} = xE_{g,ZnTe} + (1-x)E_{g,ZnSe} - bx(1-x) \quad (7)$$

where *b* is the band-bowing parameter and has an experimental value of about 1.647, $E_{g,AB}$ and $E_{g,AC}$ are the band gaps of binary compounds *AB* and *AC*, respectively. Tit *et al*. studied the origins of bandgap bowing in compound-semiconductor common-cation ternary alloys based on the sp3s* tight-binding method, and showed that the mismatch in electro-negativity between Te atom and Se atom would play a role in the bandgap bowing of alloys [13]. This can result in the valence band states lowing in energy with the increasing of Se molar fraction in the ternary alloy, while the cation Zn are contributors to the conduction band of the alloy.

3. RESULTS AND DISCUSSION

The schematic energy diagram of a ternary $ZnTe_xSe_{1-x}$/ZnTe core/shell QD under investigation is shown in figure.1. The conduction band edge of ZnTe is taken as the energy reference (i.e. E_v=0). From the diagram, it can be inferred that ZnTe has the higher valence and conduction bands than $ZnTe_xSe_{1-x}$, as Se molar fraction x is lower than the band alignment transition point (about x=0.7),

which corresponds to the classic Type-II semiconductor heterostructure. It is clearly seen that the valence band of $ZnTe_xSe_{1-x}$ bends and reduces to below the valence band bottom ZnTe as the increasing of Se molar fraction in the ternary $ZnTe_xSe_{1-x}$ core ($0.7<x<1$). The corresponding Type-I band alignment was formed, where both electron and hole were localized in the core range. The transition point between Type-I and Type-II is heavily governed by quantum confinement effect. In the following, we present the numerical results for the ternary $ZnTe_xSe_{1-x}$/ZnTe core/shell QDs. The material parameters used in calculation are listed in table 1. For the ternary semiconductor materials, all parameters were linearly interpolated for the alloys except conduction and valence energy.

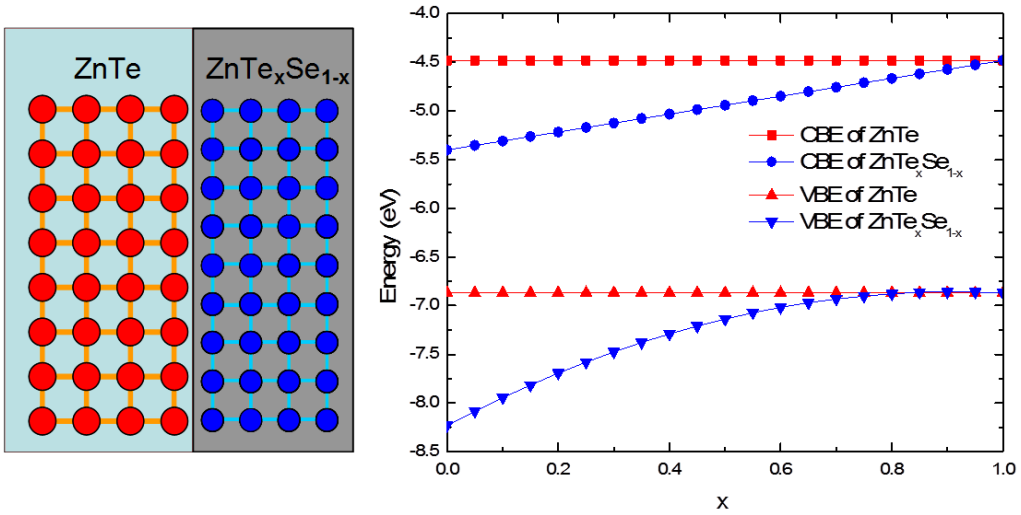

Figure 1. Band-edge alignments at the heterointerface between the ternary $ZnTe_xSe_{1-x}$ core and ZnTe shell. In the Type-II structure, the electron and hole are spatially separated in the core and shell region, respectively. In the Type-I structure, the carriers are localized in the same region.

Table 1. Material parameters for ZnTe and ZnSe.

Material	m_e/m_0	m_h/m_0	Dielectric constants	Band gap (eV)
ZnTe	0.11[15]	0.7[16]	7.78	2.39
ZnSe[3]	0.14	0.6	8.1	2.72

In order to study the effect of composition in the ternary $ZnTe_xSe_{1-x}$ core on the spatial distribution of carriers, we analyze the overlap integral between electron and hole functions defined as $\Theta = \left| \int_0^{R+H} r^2 \Re^e(r) \Re^h(r) dr \right|^2$, where r is the radial coordinate with the origin at the core center and $\Re^{e(h)}(r)$ is the radial part of the electron (hole) envelope wavefunction. Figure. 2 (left) shows the overlap integral for the different core radius as a function of the shell thickness for the fixed Se molar fraction in the ternary $ZnTe_xSe_{1-x}$ core (x=0.7). An interesting finding is that the overlap integral exhibit a transformation from type-I to type-II. It can be clearly seen that the overlap integral abruptly transit with the increasing of the core size and transformation point can mainly depend on quantum

confinement effect. Figure.2 (right) shows the exciton energy of the ground state for the ternary $ZnTe_xSe_{1-x}/ZnTe$ core/shell as a function of the shell thickness for the different core radius *r*=3, 3.5, 4, and 4.5nm, respectively. From the figure, it can importantly find that the band edge transition energy in the structure don't change abruptly with the increasing of the size of QDs, while the overlap integral change abruptly, which further indicates that the exciton energy can have a few affect due to the type-II structure forming. This shows that the size of QDs is the critical determinant of the QDs energy levels. The changing of the size of QDs can result in the variation of the band offset between the core and shell changed, which can be ascribed to the transition from type-I to type-II structure.

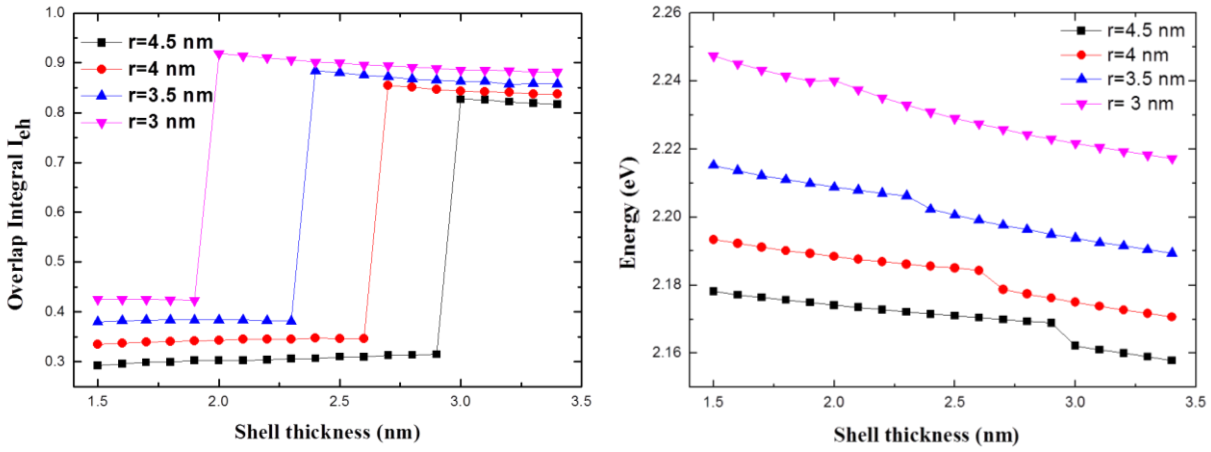

Figure 2. The calculation of the overlap integral (left) and the lowest energy 1s eigenstates (right)as a function of the shell thickness with the fixed Se molar fraction (x=0.7) in $ZnTe_xSe_{1-x}/ZnTe$ QDs for the different core size.

Figure. 3 (right) shows the ground state exciton energy in the ternary $ZnTe_xSe_{1-x}/ZnTe$ core/shell QDs as a function of the shell thickness for different Se molar fraction, i.e., *x*=0.1, 0.3, 0.5, 0.7 and 0.9, respectively. The exciton energy strongly depends on the shell thickness and the type of QDs. The dependence of energies of exciton on Se molar fraction is more obvious than on shell thickness. It is readily seen that the changing of the exciton energies of strong-confinement QDs (with large Se molar fraction) is much larger than that of weak-confinement QDs (with small Se molar fraction) in the same size of QDs. As is known to all, the carriers can appear in the region of core or shell, which mainly depend on the competition between the kinetic energy and the potential energy in the heterostrucuture QDs. According to the expression of the overlap integral, the overlap integral play an important role in carrier-carrier interaction. Thus, the QDs with large Se molar fraction results in the increasing of the overlap integral due to the strong confining of carriers (figure 3 left). This calculation also shows that shell size and composition effects significantly influence the QDs energy levels. It can be interesting to note emission peak tuning wildly and extending the emission wavelength to near-infrared wavelengths. The changing of molar fraction in the ternary $ZnTe_xSe_{1-x}$ core results in the variation of the effective masses of electron and hole, and the band offset between the core and

shell. In addition, quantum confinement effect in the ternary semiconductor compound can be the main factor of the transition from type-I to type-II structure.

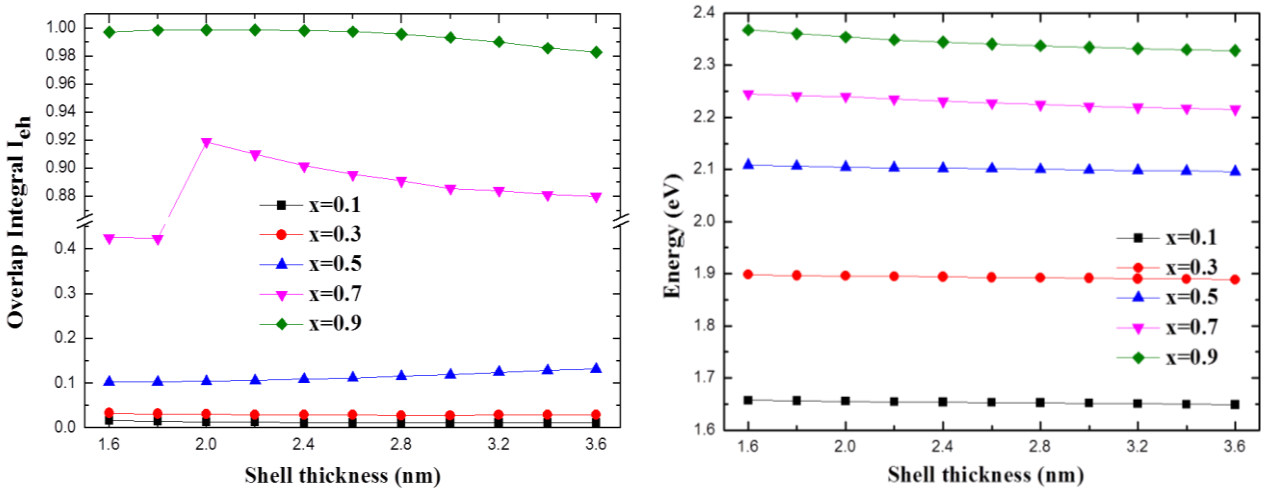

Figure 3. The calculation of the overlap integral (left) and the lowest energy 1s eigenstates (right) as a function of the shell thickness with the fixed core shell (r=3nm) in $ZnTe_xSe_{1-x}$/ZnTe QDs for the different Se molar fraction.

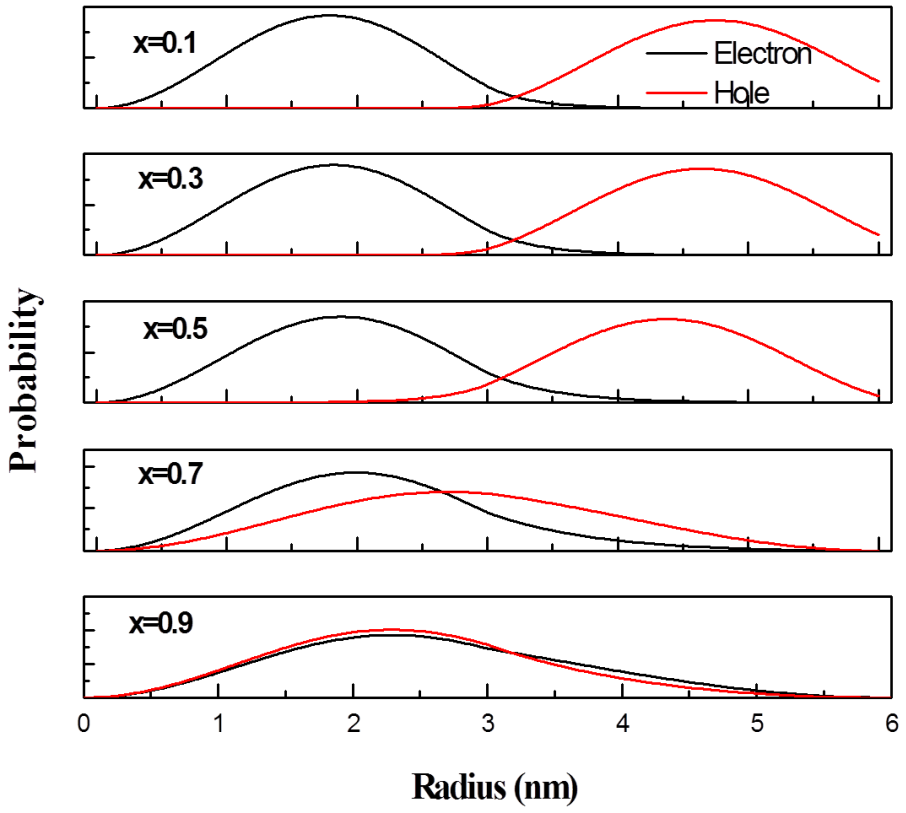

Figure 4. The probability of the presence of electron and holes in the lowest energy 1s eigenstates in $ZnTe_xSe_{1-x}$/ZnTe QDs structure with the different Se molar fraction in the ternary semiconductor core and keeping the core radius and shell size constant r=3nm, R=3nm.

According to the conduction (valence) band energy alignment between the ternary $ZnTe_xSe_{1-x}$ core and the ZnTe shell, the heterostructure types of QDs can be classified as Type-I, quasi Type-II, and Type-II with changing of the Se molar composition in QDs. We analyzes the behavior of the wavefunction of electron and hole for fixed values of the core radius and shell thickness as a function of Se molar fraction in the core in order to further understand the separation of electrons and holes in the ternary core/shell QDs. From the figure.4, it can be seen that the carrier distribution can be tuned from type-I to type-II by changing the Se molar fraction in the $ZnTe_xSe_{1-x}$ core. The electron wavefunction has a little change in the QDs with the changing of Se molar fraction, and mainly reside in the range of the core. It can be found that the distribution maxima of the electron didn't localized in the core, even though the conduction band edge of the core is lower than that of the shell, the quantum confinement effect can play an important role in the distribution of electron, especially, for the core with only 3nm radius. As the Se molar fraction changes from the 0 to 0.5, the holes primarily reside in the shell layer. The overlapping between electron and hole wavefunctions is very small, showing nearly complete spatial separation between electron and hole. The charge carriers are confined to the same range with the increasing of Se molar fraction, indicating the type-I carrier localization.

As for the regulating of the behavior of the wavefunction of electron and hole, carrier distribution can be controlled by transformation of heterostructure types of QDs from the type-I to type-II. Dong *et al* have investigated that spherical CdSe-CdS core-shell QDs are found to be flexible in the transition between the type-I regime and the type-II regime with different core/shell dimensions [14]. The electronic structure for type-II InP/GaAs quantum dot systems considering a three-dimensional geometry have been investigated by Madureira *et al* [15]. Although the number of investigation for the core/shell have been done, size effect of heterostructure type and exciton properties in $ZnTe_xSe_{1-x}$/ZnSe core/shell structure QDs is a few. The investigation can be important to realize exciton energy of the low toxicity QDs in biological window range.

4. CONCLUSIONS

In general, we study that Size effect of heterostructure type and exciton properties in a ternary $ZnTe_xSe_{1-x}$/ZnTe core/shell structure QDs, including the Coulomb interaction between electron and hole. The spatial separation between electron and hole in QDs can be presence of mutant by adjusting Se molar fraction in the core region and size of QDs. The heterostructure types of QDs can be changed from Type-I, to Type-II with changing of the size of QDs, which can be ascribed to size effect, which show that the quantum confinement effect in the ternary core is a key to the transformation from the type-I to type- II. It is also found that the 1*s* transition energies depend sensitively on the core radius of the QDs and Se molar fraction in the ternary core.

ACKNOWLEDGEMENTS

This work has been partly supported by the National Key Basic Research Program of China (2012CB934201), the National Natural Science Foundation of China (11147024, 11247025, and 11074129).

References

1. Drbohlavova Jana, Chomoucka Jana, Hrdy Radim, *Int. J. Electrochem. Sci.*,7(2012) 1424-1432
2. Shen Xiaofang, Li Zhaoxia, Cui Yan, *Int. J. Electrochem. Sci.*,6(2011) 3525-3535
3. Hamizi Nor Aliya, Ying Ch'ng Shiau, Johan Mohd Rafie, *Int. J. Electrochem. Sci.*,7(2012)4727-4734
4. Rad Ali Shokuhi, Mirabi Ali, Binaian Ehsan, *Int. J. Electrochem. Sci.*,6(2011) 3671-3683
5. Ndangili Peter M, Olowu Rasaq A, Mailu Stephen N, *Int. J. Electrochem. Sci.*,6(2011) 1438-1453
6. S.A. Ivanov, A. Piryatinski, J. Nanda, S. Tretiak, K. R. Zavadil, W. O. Wallace, D. Werder, V.I. Klimov, *J. Am. Chem. Soc.*, 129 (2007) 11708-11719
7. Jia Guo-zhi, Wang Yun-feng, Gong Lei, Digest *Journal of Nanomaterials and Biostructures*, 6(2011)43-53
8. J. He, C. J. Reyner, B. L. Liang, K. Nunna, D. L. Huffaker, N. Pavarelli, K. Gradkowski, T. J. Ochalski, G. Huyet, V. G. Dorogan, Yu. I. Mazur, G. J. Salamo, *Nano Lett.* 10(2010)3052–3056
9. Oron D., Kazes M., Banin U., *Physical Review B*, 75(2007)115333
10. Jia Guo-zhi, Wang Yun-feng, Yao Jiang-hong, *Optoelectronics and Advanced Materials-rapid Communications*, 4(2010) 2080-2084
11. Chang K., Xia J. B., *Physical Review B*, 57(1998) 9780-9786
12. Jia Guo-zhi, *Optoelectronics and Advanced Materials-rapid Communications*, 5(2011) 738-741
13. Tit N., Obaidat I. M., Alawadhi H., *Journal of Physics-Condensed Matter* 21(2009) 273:478
14. Lin Dong, Abhilash Sugunan, Jun Hu, Sicheng Zhou, Shanghua Li, Sergei Popov, Muhammet S. Toprak, Ari T. Friberg, Mamoun Muhammed, *Applied Optic*s, 52(2013)105.
15. Justino R. Madureira, Márcio P. F. de Godoy, Maria J. S. P. Brasil, Fernando Iikawa, *Appl Phys Lett*, 90(2007) 212105.